

## Article

# Assessing Future Impacts of Climate Change on Streamflow within the Alabama River Basin

Joseph E. Quansah <sup>1,\*</sup>, Amina B. Naliaka <sup>2</sup>, Souleymane Fall <sup>1</sup>, Ramble Ankumah <sup>1</sup> and Gamal El Afandi <sup>1</sup> 

<sup>1</sup> Department of Agricultural and Environmental Sciences, Tuskegee University, Tuskegee, AL 36088, USA; sfall@tuskegee.edu (S.F.); rankumah@tuskegee.edu (R.A.); gelafandi@tuskegee.edu (G.E.A.)

<sup>2</sup> School of Earth Systems and Sustainability, Southern Illinois University, Carbondale, IL 62901, USA; amina.naliaka@siu.edu

\* Correspondence: jqansah@tuskegee.edu; Tel.: +1-3347278419

**Abstract:** Global climate change is expected to impact future precipitation and surface temperature trends and could alter local hydrologic systems. This study assessed the likely hydrologic responses and changes in streamflow due to future climate change within the Alabama River Basin (ARB) for the mid-21st century 2045 (“2030–2060”) and end-21st century 2075 (“2060–2090”). Using an integrated modeling approach, General Circulation Model (GCM) datasets; the Centre National de Recherches Météorologiques Climate Model 5 (CNRM-CM5), the Community Earth System Model, version 1–Biogeochemistry (CESM1- BGC.1), and the Hadley Centre Global Environment Model version 2 (HADGEM2-AO.1), under medium Representative Concentration Pathway (RCP) 4.5, and based on World Climate Research Program (WCRP)’s Couple Model Intercomparison Phase 5 (CMIP5), were assimilated into calibrated Soil and Water Assessment Tool (SWAT). Mann–Kendall and Theil Sen’s slope were used to assess the trends and magnitude of variability of the historical climate data used for setting up the model. The model calibration showed goodness of fit with minimum Nash–Sutcliffe Efficiency (NSE) coefficient values of 0.83 and Coefficient of Determination ( $R^2$ ) of 0.88 for the three gages within the ARB. Next, the research assessed changes in streamflow for the years 2045 and 2075 against that of the reference baseline year of 1980. The results indicate situations of likely increase and decrease in mean monthly streamflow discharge and increase in the frequency and variability in peak flows during the periods from the mid to end of the 21st century. Seasonally, monthly streamflow increases between 50% and 250% were found for spring and autumn months with decreases in summer months for 2045. Spring and summer months for 2075 resulted in increased monthly streamflow between 50% and 300%, while autumn and spring months experienced decreased streamflow. While the results are prone to inherent uncertainties in the downscaled GCM data used, the simulated dynamics in streamflow and water availability provide critical information for stakeholders to develop sustainable water management and climate change adaptation options for the ARB.

**Keywords:** climate change; streamflow; SWAT model; GCM; CNRM-CM5; CESM1-BGC.1; HADGEM2-AO.1; Alabama River Basin



**Citation:** Quansah, J.E.; Naliaka, A.B.; Fall, S.; Ankumah, R.; Afandi, G.E. Assessing Future Impacts of Climate Change on Streamflow within the Alabama River Basin. *Climate* **2021**, *9*, 55. <https://doi.org/10.3390/cli9040055>

Academic Editor: Ying Ouyang

Received: 5 February 2021

Accepted: 26 March 2021

Published: 31 March 2021

**Publisher’s Note:** MDPI stays neutral with regard to jurisdictional claims in published maps and institutional affiliations.



**Copyright:** © 2021 by the authors. Licensee MDPI, Basel, Switzerland. This article is an open access article distributed under the terms and conditions of the Creative Commons Attribution (CC BY) license (<https://creativecommons.org/licenses/by/4.0/>).

## 1. Introduction

According to the United Nations Framework Convention on Climate Change [1], climate change could be defined as “a change of climate which is attributed directly or indirectly to human activity that alters the composition of the global atmosphere and which is in addition to natural climate variability observed over comparable time periods” [1]. Climate change may be due to natural internal processes or external forcings, such as modulations of the solar cycles, volcanic eruptions, and persistent anthropogenic changes in the composition of the atmosphere or inland use [2]. The latest Intergovernmental Panel on Climate Change (IPCC) assessment reports show global climate change as a scientific

reality and one of the most significant challenges facing humanity today [3]. Climate change is mainly manifested by the change in global mean surface temperatures.

Temperature data from several scientists and organizations show that global climate warming trends have been increasing rapidly in the past few decades [4]. Globally, nineteen of the twenty warmest years all have occurred since 2001, except for 1998, with 2016 being the warmest on record since 1880 [5]. The 10 warmest years in the 140-year record all have occurred since 2005, with the six warmest years being the six most recent years [4]. The ten warmest Augusts have all occurred since 1998, and the five warmest have occurred since 2015 [4]. Averaged as a whole, the August 2020 global land and ocean surface temperature was 0.94 °C (1.69 °F) above average, and the second highest August temperature since 1880 [3]. According to National Oceanic and Atmospheric Administration (NOAA) (2020), both August 2020 global land-only and 2016 ocean-only surface temperatures were among the highest ever recorded, at 1.26 °C (2.27 °F) and 0.82 °C (1.48 °F) above average, respectively [4]. Human-induced global warming reached approximately 1 °C above pre-historic levels in 2017 and is projected to reach to 1.5 °C above pre-industrial levels by 2040 [6]. Rising sea surface temperatures have resulted in increases in tropical storms and hurricanes [7]. Additionally, global average sea levels are projected to continue to rise (approximately 7.2 to 23.6 inches/18–59 cm/0.18–0.59 m) by the end of the century [8]. All these facts add credence to the IPCC's conclusion that climate change is real, will continue to increase in severity, and requires human and governmental actions to control the current trends.

Historically, increases in surface temperature have resulted in changes in the intensity spatial distribution, and temporal trends in precipitation, and have subsequently impacted different regional and local hydrologic systems around the world [7,9]. Climate change is expected to modify the hydrologic cycle and has significant implications for water resources. These include observed increased evaporation rates, a higher proportion of precipitation received as rain rather than snow, earlier and shorter runoff seasons, changes in water budget and streamflows, increased water body temperatures, such as the warming of lakes and rivers, and decreased water quality in both inland and coastal areas [10–12]. Impacts of climate change on freshwater ecosystems also include observed changes in species composition, organism abundance, productivity, and phenological shifts [13]. Aquatic habitats, as well as water quality, have been negatively affected, resulting in lower levels of dissolved oxygen, increases in pollutants, pathogens, nutrients, and invasive species as well as algal blooms [10,11,14]. Additionally, there have been losses and changes in the distribution of aquatic species with higher rates of evapotranspiration resulting in some water bodies shrinking [12].

Variability in precipitation relative to evaporation and increasing surface temperatures cause changes in residence time, water budget, and water temperature dynamics of lakes, streams, rivers, and other water bodies [15]. Temporal and spatial variabilities in precipitation intensity have the potential to cause shifts in the connectivity of water bodies as well as in erosion rates that could affect the inflow and outflow dynamics of various water bodies for different regions [15]. For instance, according to the United States Environmental Protection Agency (U.S. EPA) during the past 75 years, seven-day low flow has generally increased in the Northeast and Midwest regions of the United States while parts of the Southeast and the Pacific Northwest regions have generally had decreases in low flows [16,17]. Moreover, three-day high-flow trends have varied from region to region across the U.S., with high flows observed to have generally increased or changed little in the Northeast since 1940, while high flows have also increased in some West Coast streams and decreased in others [16,17]. Annual average streamflow has increased at many sites in the Northeast and Midwest, while other regions have seen few substantial changes [16,17]. Net water supplies have increased in areas with sufficient rainfall while certain areas have experienced long droughts and decreases in net water supply [17,18]. This decrease is partly due to the temperature rise and associated increase in evaporation rates in most areas [17,18]. Parametric and nonparametric-based assessment of historical long-term trends and seasonal variability in streamflow have shown increasing and decreasing flow

trends for different hydrologic regions [19,20]. Regions experiencing a decline in the water supply are likely to experience an increase in water demand because of the increasing population. The decrease in water supply could be particularly significant for agriculture, energy production, municipal, industrial, and other uses [21]. Changes in the timing, intensity, and duration of precipitation negatively affect water quality. As a result of increased rainfall and intense rainstorms, flooding and surface runoff transport large volumes of water and contaminants into water bodies. Intense flooding events can also overwhelm water infrastructures including storm, combined sewer, and wastewater systems, causing untreated pollutants to directly enter and contaminate source water supply systems. In regions with increased rainfall frequency and intensity, more pollution and sedimentation might result from runoff. On the other hand, reduced rainfall and increased temperatures will result in drier soils and lead to increasing incidences of wildfires making land more vulnerable to soil erosion [22]. Increasing occurrences of tropical storms will result in increased flooding which may consequently damage infrastructure and lead to coastal erosion [23]. Climate change has adversely impacted food security and terrestrial ecosystems as well as contributed to desertification and land degradation in many regions [3]. Sustainable land management, including sustainable forest management, can prevent and reduce land degradation, maintain land productivity, and sometimes reverse the adverse impacts of climate change on land degradation, while contributing to mitigation and adaptation solutions [3].

To effectively assess future hydrologic responses to climate change, scientists utilize hydrologic modeling integrated with future projected climate dataset derived from the World Climate Research Program (WCRP) and IPCC's General Circulation Models (GCMs). The GCMs are the most advanced tools for simulating the response of the global climate system to increasing greenhouse gas concentrations [23]. GCMs provide geographically and physically consistent estimates of future regional climate conditions and changes throughout the planet based on physical processes involving the atmosphere, ocean, and land surface [23,24]. The latest GCM dataset is the WCRP's Coupled Model Intercomparison Project Phase 6 (CMIP6). These new generation climate models have resulted in significant improvements in the knowledge and understanding of future climate variability and change. Greenhouse gas emission scenarios are the primary radiative forcing that drive the GCMs. There are a standard set of scenarios for future global greenhouse gas emissions based on land use, population growth, technology, industrialization, and other factors that are employed by climate modelers [23]. These are the Representative Concentration Pathways (RCPs), and are expressed as the amount, by the year 2100, of the earth's radiative imbalance in watts per square meter of earth's surface. RCPs were introduced in the Fifth IPCC Assessment and are used to prescribe radiative forcing inputs to climate models [23,25–27]. The four standard RCPs are RCP2.6, RCP4.5, RCP6.5, and RCP8.5, which represent increases of +2.6, +4.5, +6.5, and +8.5 watts per square meter ( $W/m^2$ ), respectively. The RCP 2.6 scenario is a relatively low greenhouse-gas emission scenario, while RCP 4.5, RCP 6.5, and RCP 8.5 appear as reasonable choices to represent medium to high stabilization radiative forcing emission scenarios [23]. As an integral part of assessing impacts of climate change on hydrologic systems, downscaled GCM data under various RCP scenarios are assimilated into hydrologic models to simulate past, current, and future hydrologic processes, and responses to different climate conditions [28–31]. Due to spatial scales and inherent uncertainties in downscaled GCM datasets integrated into hydrologic models, there could be substantial variability in simulated hydrologic outputs and responses to climate change [32].

The State of Alabama, in the southern U.S., has experienced over the years periods of flooding and low flows as a result of changing climate. For instance, in 1990, the Alabama River flooded homes in Selma and Montgomery, while in 2007 and 2016 severe drought hit the region. Reduced runoff and lower groundwater levels in the summer could impact water availability to satisfy Alabama's growing and competing needs for municipal, industrial, agricultural irrigation, and recreational uses of water [33]. Large groundwater

withdrawals in the coastal zones of Baldwin and Mobile counties, which include the Mobile Bay and Gulf Shores regions, have increased salinity in wells due to saltwater intrusion into the aquifers [34]. An increase in sinkhole formation has also been associated with growing groundwater withdrawals [35]. Warmer and drier conditions, particularly if accompanied by rising sea levels, could compound these types of problems due to higher demand and lower flows. Lower flows and higher temperatures could also degrade water quality by concentrating pollutants and reducing the assimilation of wastes [33]. One of the largest off-stream uses of water in Alabama is thermoelectric power generation. Higher water temperatures could reduce the efficiency of industrial and power plant cooling systems and might make it increasingly difficult to meet regulatory standards for acceptable downstream water temperatures, particularly during extremely warm periods. Increases in precipitation would alleviate these impacts. However, higher rainfall, particularly during the traditional winter-spring flood season, could contribute to localized flooding and increased levels of pesticides and fertilizers in runoff from agricultural areas [33]. Historically, Alabama experienced the hottest temperatures in the 1920s and 1930s, followed by a substantial cooling of almost 2 °F into the 1960s and 1970s. Since that cool period, temperatures have risen by about 1.5 °F, such that the most recent decades have experienced records above the long-term average, but slightly cooler than the 1920s/1930s [36]. Because of the large cooling that occurred in the middle of the 20th century, the southeastern United States is one of the few regions globally that has not experienced overall warming since 1900, while the United States as a whole has warmed by about 1.5 °F. In the summer, daytime high temperatures have typically ranged between 85 °F and 95 °F, with temperatures regularly exceeding 95 °F across the state [36].

Under a higher emissions pathway, historically unprecedented warming is projected by the end of the 21st century. Even under a lower pathway of greenhouse gas concentrations, temperatures are projected to exceed historical record levels by the middle of the 21st century. However, there is a large range of temperature increases projected under both pathways, and under the lower pathway, a few projections are slightly warmer than historical records [36]. Warming is projected despite the lack of a long-term temperature trend in Alabama because the increased warming influence of greenhouse gases is expected to become greater than the natural variations that have dominated Alabama's temperatures [36]. Future changes in average annual precipitation are uncertain. However, any increase in temperature will cause a more rapid rate of loss of soil moisture during dry periods. This will likely increase the intensity of naturally occurring droughts in the future. Increases in extreme precipitation are projected for Alabama because it is virtually certain that atmospheric water vapor will increase in a warmer world [36,37]. Therefore, both droughts and wetter episodes are expected to occur, and this increase in various types of extreme climatic events is one of climate change hallmarks [38].

Because of the above observations, it is critical to assess future climate change impacts on hydrologic systems and water resources. The objective of the study was to assess the likely hydrologic responses and changes in mean monthly streamflow discharge due to future climate change within the Alabama River Basin (ARB), for the mid (2030–2060) and end (2060–2090) of the 21st century. The integrated modeling approach used involved the assimilation of the three best performing downscaled CMIP5 GCM data, namely the Centre National de Recherches Météorologiques Climate Model 5 (CNRM-CM5), the Community Earth System Model, version 1–Biogeochemistry (CESM1-BGC.1), and the Hadley Centre Global Environment Model version 2 (HADGEM2-AO.1), under medium emission scenario (RCP 4.5) into the Soil and Water Assessment Tool (SWAT) to simulate monthly streamflow variability and magnitude for the years 2045, representing the mid-21st century ("2030–2060"), and 2075, representing the end-21st century ("2060–2090"). The results from this study together with the relevant knowledge about the Alabama River Basin, and other related research studies would provide critical information for the development of climate change adaptation solutions to ensure sustainable management of water resources within the Alabama River Basin and the southeastern USA in general.

## 2. Materials and Methods

### 2.1. Study Area

The study area is the Alabama River Basin (ARB), which consists of Alabama, Coosa, Tallapoosa, and Cahaba River Basins (Figure 1). The ARB covers the northwestern part of Georgia and enters through northeastern Alabama, covering a region which includes the central and southeastern Alabama and covers a total drainage area of approximately 59,051 km<sup>2</sup> [39]. The headwater streams of the ARB river basin rise in the Blue Ridge Mountains of Georgia and Tennessee and flow southwest, combining at Rome, Georgia, to form the Coosa River [39]. The confluence of the Coosa and Tallapoosa Rivers in central Alabama forms the Alabama River, which flows through Montgomery and Selma. The Alabama River then joins with the Tombigbee River at the bottom of the ARB about 45 miles north of Mobile to form the Mobile River, which flows into Mobile Bay at an estuary of the Gulf of Mexico [39]. The ARB contributes 33,600 ft<sup>3</sup>/s (951.5 m<sup>3</sup>/s) of streamflow to the Mobile River [39].

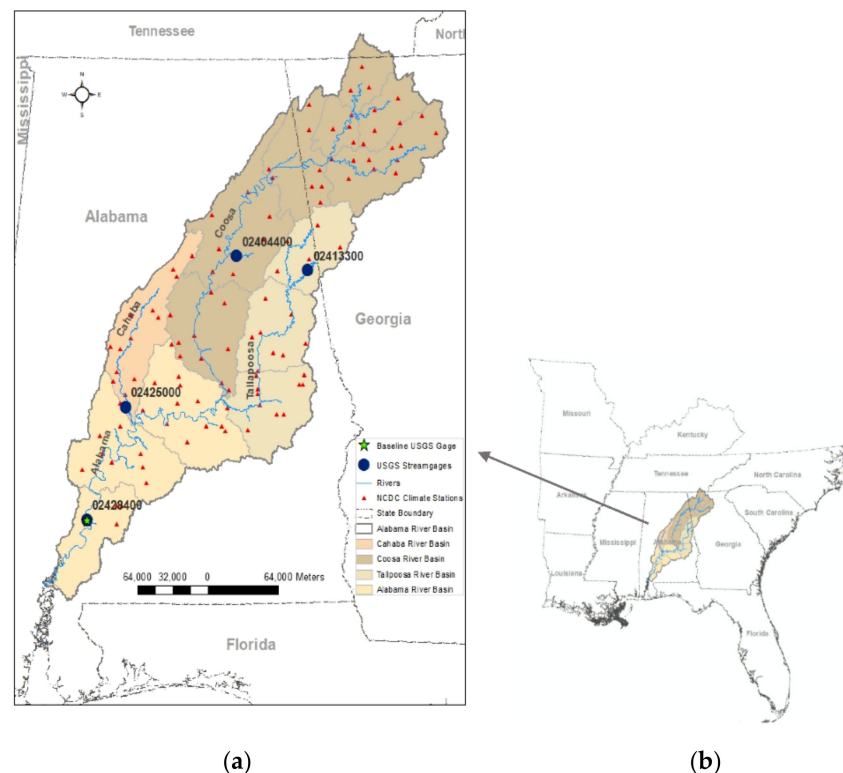


**Figure 1.** The study area: (a) the major basins, climate stations, and U.S. Geological Survey (USGS) gages; (b) location of the basin within Alabama and southeastern U.S.

The state of Alabama has a humid, subtropical climate, with mild winters and hot summers. Extreme temperatures range from near 110 °F in the summer to values below zero in the winter [39]. In the southern end of the basin, the average maximum January temperature is 60 °F, and the average minimum January temperature is 37 °F [39]. The maximum average July temperature is 91 °F; in the southern end of the basin, the corresponding minimum value is 69 °F [39]. The frost-free season varies in length from about 200 days in the northern valleys to about 250 days in the southern part of the basin [39]. The ARB has elevation that ranges from sea level to 1278 m and has soil type consisting mainly of sandy loam and silty loam [40]. The average annual precipitation for the ARB is 1379 mm, mainly from rainfall and limited contributions from snowfall [40]. The dominant land use types for the ARB are forestry (about 73%) and agriculture (about 17%), consisting mainly of hay/pasture, corn, cotton, peanuts, and soybean. The large forest land cover results in

high evapotranspiration ranging from 762 to 1067 mm (56–78% of annual precipitation), generally increasing from north to south [40].

## 2.2. Soil and Water Assessment Tool

The Soil and Water Assessment Tool (SWAT) is an ecohydrological model developed by the United States Department of Agriculture (USDA)–Agricultural Research Service (ARS) [41]. SWAT is a continuous-time, semi-distributed, dynamic, and spatially distributed model, based on mathematical descriptions of physical, biogeochemical, and hydrochemical processes in simulating hydrologic processes, streamflow, impacts of land use and agricultural management practices on water quality, the fate and transport of pollutants, sediment, and agricultural chemical yields, at various watershed scales [41,42]. The major model components are weather conditions, hydrology, soil properties, plant growth, and land management, as well as loads and flows of nutrients, pesticides, bacteria, and pathogens. SWAT can simulate major hydrologic processes including evapotranspiration (ET), surface runoff, infiltration, percolation, shallow aquifer, and deep aquifer flow, and channel routing [41]. Moreover, [43] provide details and the theoretical background of the SWAT model. The SWAT model is one of the most widely used hydrologic and water quality models worldwide and can be applied across a range of watershed scales, climatic zones, environmental conditions, and management systems extensively for a broad range of hydrologic and/or environmental studies and decision making [42]. The international use of SWAT has mostly been attributed to its flexibility in addressing water resource problems.

## 2.3. General Circulation Models and Uncertainties

Although CMIP5 GCMs have been widely applied in the assessment of hydrologic responses to climate change, there are uncertainties associated with outputs of GCMs. According to [44], the greatest source of uncertainty is the large spatial and temporal scale of GCMs. This gives rise to another source of uncertainty: the downscaling techniques that are necessary to convert GCM model outputs to scales that are useful for most hydrological modeling applications [23]. Another critical source of uncertainty in GCM is the accuracy in the projections of drought conditions. According to [45], uncertainties in projected drought scenarios could contribute as high as 97% to total uncertainty in climate models. Research work by [46] projected that, while precipitation is likely to increase in the 21 century, frequencies in droughts are expected to increase by between 10% and 50% over most land areas.

Therefore, there are different levels of uncertainties depending on the accuracy of the downscaled GCM data and the RCP greenhouse gas emission scenarios being used. Several researchers have been able to assess climate change impact across a range of spatial and temporal scales using GCM data that most accurately simulate historical climate conditions of their study areas [24,29,31]. RCP 4.5 and 8.5 are identified as conservative and severe, respectively in CMIP5 projections to demonstrate the sensitivity of Midwestern U.S. watersheds to future climatic changes [31].

In this study, we considered the top three CMIP5 GCMs climate data recommended for southeastern United States (U.S.) by U.S. Geological Survey (USGS). USGS evaluated CMIP5 GCMs concerning how well they reproduced the observed climate of the Southeastern U.S. Monthly data (temperature and precipitation) from 41 GCMs of the CMIP5 were compared to observations for the 20th century for the Southeastern United States and surrounding areas. They utilized a suite of statistics/metrics that characterize various aspects of the regional climate. Each GCM's performance was then assessed and ranked, based on its ability to reproduce the observed climatic variables [47]. Overall, the highest-ranked models included the CNRM-CM5/CNRM-CM5-2 pair of models, the CESM1/CCSM4 family of models (except for CESM1-WACCM), and the CMCC-CM/CMCC-CMS pair of models. Other high scoring models are MPI-ESM-LR, the "CC" versions of the GISS family of models, and HadGEM2-ES. For this study CNRM-CM5 [48], CESM1-BGC.1 [49], and

HADGEM2-AO.1 [50] model data, under medium stabilization radiative forcing emission scenario (RCP4.5), were selected based on their performance as compared to observation data for the research watershed for the years between 1980 and 2010.

#### 2.4. Historical and Future Climate Scenario Data

This study utilized historical climate and streamflow data (1980–2010) and statistically downscaled GCM CMIP5 climate data (daily precipitation, minimum and maximum temperatures) for the years 2045 (representing the mid-21st century (2030–2060) and 2075 (representing the end-21st century (2060–2090)), under medium stabilization radiative forcing emission scenario (RCP4.5). The historical data were used together with other watershed and geospatial data to set up, calibrate, and validate the SWAT model. The downscaled future climate data were assimilated into calibrated SWAT models to simulate and analyze the dynamics of future streamflow for selected GCMs under RCP4.5 scenario. A detailed description of the scenario is provided by [51]. Data from CNRM-CM5 [48], CESM1-BGC.1 [49], and HADGEM2-AO.1 [50] models were used in this study. The data (1/16° resolution) were obtained from [http://gdo-dcp.ucllnl.org/downscaled\\_cmip\\_projections/](http://gdo-dcp.ucllnl.org/downscaled_cmip_projections/) (accessed on 2 July 2018) [52]. The different GCM simulations were run and assessed on monthly time steps, from January 1 to December 31 for the years 2045 and 2075, to evaluate future changes in streamflow dynamics and water availability. Streamflow projections from the different models were then compared to those for the baseline year of 1980 to assess climate change impacts.

#### 2.5. Hydrologic Modeling Data

The data used as input for the SWAT model included the USDA National Elevation Data (NED), historical climate, streamflow, water quality, USDA National Agricultural Statistics Service (NASS) cropland, State Soil Geographic (STATSGO), and downscaled GCM data. The data used, sources, and description are as shown in Table 1.

**Table 1.** Table showing geospatial and climate data and sources.

Data	Data Source	Data Description
Elevation (30 m)	United States Department of Agriculture Geospatial Data Gateway <a href="http://datagateway.nrcs.usda.gov">http://datagateway.nrcs.usda.gov</a>	National Elevation Dataset
State Soil Geographic data	United States Department of Agriculture Geospatial Data Gateway <a href="http://datagateway.nrcs.usda.gov">http://datagateway.nrcs.usda.gov</a>	Soil classification and properties
Land Use (30 m)	United States Department of Agriculture Geospatial Data Gateway <a href="http://datagateway.nrcs.usda.gov">http://datagateway.nrcs.usda.gov</a>	National Land Cover Dataset Land
Historical Climate	National Climatic Data Center <a href="http://www.ncdc.noaa.gov/cdo-web">http://www.ncdc.noaa.gov/cdo-web</a>	Daily rainfall, maximum and minimum temperature
Streamflow	United States Geological Survey Water Data <a href="https://waterdata.usgs.gov/nwis">https://waterdata.usgs.gov/nwis</a>	Monthly streamflow
Future Climate	<a href="http://gdo-dcp.ucllnl.org/downscaled_cmip_projections/">http://gdo-dcp.ucllnl.org/downscaled_cmip_projections/</a>	Downscaled General Circulation Model data for 2045 and 2075

#### 2.6. SWAT Model Setup, Calibration, and Validation Analysis

The geospatial data were processed and assimilated into the SWAT model. An initial cold/default simulation was run to obtain the initial performance of the model, which then served as the basis for the calibration of long-term water balance [53]. The model was then calibrated, validated, and assessed for performance accuracy and efficiency.

According to [54], calibration is the process that involves the effort to parameterize a model to a given set of local conditions, thereby reducing the prediction uncertainty. Nash–Sutcliffe Efficiency (NSE) coefficient [55] (Equation (1)) and the Coefficient of Determination ( $R^2$ ) (Equation (2)) statistics were used to assess the performance of the SWAT model. The

NSE is commonly used to assess the predictive performance of hydrologic models and has values ranging from  $-\infty$  to 1. A hydrologic model is considered as having optimal performance if NSE values are above 0.5, with a 1 indicating a perfect match of model simulation with measured data [56].  $R^2$  represents the correlation between the simulated and measured data, with values ranging between 0 and 1, where 0 corresponds to no correlation and 1 indicates a perfect correlation [56]. A high  $R^2$  value may not necessarily be an indication of an acceptable model performance or efficiency [57,58]. A good assessment of the acceptability of  $R^2$  value, is to make graphical comparison of the series scatter plots to ensure their closeness to the 1:1 ratio line and also observe the good-of-fit of the resulting hydrographs of simulated and measured data. Generally,  $R^2$  values are higher than corresponding NSE values.

Measured data from three USGS gages (02404400, 02413300, and 02425000) were used for monthly calibration for the period 1995–2005, and monthly validation was performed for the period 1985–1995. The hydrologic parameters that were systematically changed in the calibration included initial SCS runoff curve number for moisture condition II (CN2), soil evaporation compensation factor (ESCO), available water capacity of first soil layer (mm/mm) (SOL\_AWC), baseflow alpha factor (days)(ALPHA\_BF), threshold depth of water in the shallow aquifer for return flow to occur (mm H2O) (GWQMIN) and groundwater "revap" coefficient (GW\_REVAP).

$$NSE = 1 - \frac{\sum_{i=1}^n (O_i - P_i)^2}{\sum_{i=1}^n (O_i - O_{avg})^2} \tag{1}$$

$$R^2 = \left[ \frac{\sum_{i=1}^n (O_i - O_{avg})(P_i - P_{avg})}{\sqrt{\sum_{i=1}^n (O_i - O_{avg})^2 \sum_{i=1}^n (P_i - P_{avg})^2}} \right]^2 \tag{2}$$

where,  $n$  is the total number of observations or simulation;  $i$  is number of values,  $O$  is measured values;  $P$  is predicted or simulated output values.

### 2.7. Climate Trend Analysis

The time series of the historical climate data for the period between 1980 and 2010 was analyzed for temporal variability trends using the non-parametric Mann–Kendall method [59] and the magnitude of the trends was determined using Theil Sen’s slope estimator [60,61]. Trend analysis was performed to quantify the rate of change, the magnitude of trend, the sign (increase or decrease) in change and whether the change in the annual rainfall and temperature was statistically significant. The trend test was positive (increasing) for precipitation and minimum temperature and non-null for maximum temperature (Table 2). All three climate variables showed little to no observable long-term variation over the historical period between 1980 and 2010.

**Table 2.** Mann–Kendall Trend Test Results.

Variable	Number of Years	Mann–Kendall	Trend
Precipitation	30	+	1
Maximum Temperature	30	+	0
Minimum Temperature	30	+	1

### 2.8. Analysis of Simulated Baseline versus Future Streamflow Discharge

To study streamflow changes resulting from projected climate change, streamflow discharge and hydrographs for the historical baseline year of 1980 were analyzed against those under future climate conditions for the mid (2045) and end (2075) of the 21st century. The time series of total streamflow discharge for projected climate conditions under the

selected climate scenario were analyzed for changes against that for baseline periods. To achieve this, measured streamflow from the USGS gage closest to the watershed outlet (USGS gage 02428400 in Figure 1) was utilized because there was no USGS gage at the main watershed outlet. The simulated average streamflow based on historical climate data for the baseline periods were compared to the simulated streamflow for future climate conditions, mainly to determine the changes in streamflow discharge values and trends in peak flow variabilities that could occur within the study area for the years 2045 and 2075.

### 3. Results and Discussion

#### 3.1. Comparison of GCM Climate Variables with Observed Baseline Values

The selected GCMs predicted changes in average daily maximum temperature ranging between 24.29 °C and 27.42 °C, average daily minimum temperatures between 11.33 °C and 14.75 °C, and average daily precipitation between 3.62 and 3.99 mm for 2045. Predictions for 2075 showed changes ranging between 3.63 and 4.48 mm for average daily precipitation, 24.30 °C–27.98 °C for average daily maximum temperature, and 11.32 °C–14.62 °C for average minimum daily temperature. CESM1-BGC.1 predicted an increase in average daily precipitation, while HADGEM2-AO and CNRM-CM5 predicted decreases in average daily precipitation for 2045 compared to the 1980 baseline values. For 2075, both CESM1-BGC.1 and HadGEM2-AO.1 had predictions above the 1980 baseline value while CNRM-CM5 prediction was below the 1980 baseline value. CESM1-BGC.1 and HadGEM2-AO.1 predicted a rise in average daily minimum and maximum temperatures above the baseline temperatures years for both 2045 and 2075. CNRM-CM5 predicted a decrease in average daily maximum temperature for both 2045 and 2075 compared to 1980 baseline values and an increase in average minimum temperatures for both 2045 and 2075. The CNRM-CM5 model projected the lowest change in both temperature and precipitation while HADGEM2-AO projected the largest increase change for both climate variables. The summary of the daily average values and change statistics for historical baseline and projected climatic variables are shown in Table 3.

**Table 3.** GCM projected average daily climatic variables and percentage change to 1980 baseline values.

Climate Data Type	Precipitation (mm/day)	Precipitation Change (%)	Maximum Temperature (°C)	Maximum Temperature Change (%)	Minimum Temperature (°C)	Minimum Temperature Change (%)
Baseline_1980	3.93		24.42		10.69	
CNRM-CM5_2045	3.62	−7.89	24.29	−0.53	11.33	5.99
CESM1-BGC.1_2045	3.99	1.53	27.42	12.29	14.75	37.98
HADGEM2-AO.1_2045	3.91	−0.509	26.89	10.11	13.46	25.91
CNRM-CM5_2075	3.63	−7.63	24.3	−0.49	11.32	5.89
CESM1-BGC.1_2075	3.99	1.53	26.47	8.39	13.25	23.95
HADGEM2-AO.1_2075	4.48	13.99	27.98	14.58	14.62	36.76

#### 3.2. SWAT Model Calibration, Validation Results and Performance

Calibration and validation processes were performed to ensure acceptable performance efficiency for the SWAT model. Measured streamflow data for USGS gage stations 02404400, 02413300, and 02425000 were used to calibrate (1995–2005) and validate (1985–1995) the SWAT model. Six sensitive parameters were modified to calibrate total streamflow, surface runoff, and baseflow. The calibrated parameters included CN2, ESCO, SOL\_AWC, ALPHA BF, GWQMN, and GW\_REVAP (Table 4). The calibrated model was further validated for the period 1985–1995. Statistical results for the monthly simulation

calibration and validation processes for the different gage stations within the watershed are listed in Table 5. For the calibration period, the SWAT simulated flow fitted well with the observed data. The resulting NSE values ranged between 0.83 and 0.89,  $R^2$  values ranged between 0.88 and 0.90 for the calibration period; NSE for the validation period ranged from 0.78 to 0.94, and the  $R^2$  ranged from 0.85 to 0.94. Figures 2 and 3 show the scatter plots and results of the objective functions for all three gages used for the calibration and validation.

**Table 4.** Default and calibrated Soil and Water Assessment Tool (SWAT) variables values used in the study.

Streamflow Calibration	Component Variables	Description of Variables	Default Value	Calibrated Value	Input File
Surface	CN2	SCS runoff curve number for moisture condition II	27–94	Reduced by 4 for all sub-basins	.mgt
	ESCO	Soil evaporation compensation factor	0.95	0.90	.bsn
	SOL_AWC	Soil available water capacity	0–0.35	Increased by 0.2	.sol
Baseflow	ALPHA_BF	Groundwater recession factor	0.048d	replaced with 0.3	.gw
	GW_REVAP	Groundwater revap coefficient	0.02	increased by 0.1	.gw
	GWQMIN	Threshold depth of water in the shallow aquifer required for return flow to occur	1000	800	.gw

**Table 5.** Model performance statistics for streamflow calibration and validation.

Station Location	USGS Gage No.	Drainage Area (km <sup>2</sup> )	Calibration		Validation	
			$R^2$	NSE	$R^2$	NSE
Choccolocco Creek at Jackson Shoal near Lincoln	2404400	1245	0.88	0.87	0.92	0.92
Little Tallapoosa River near Newell	2413300	1050	0.90	0.82	0.85	0.78
Cahaba River near Marion Junction	2425000	4567	0.90	0.89	0.94	0.94

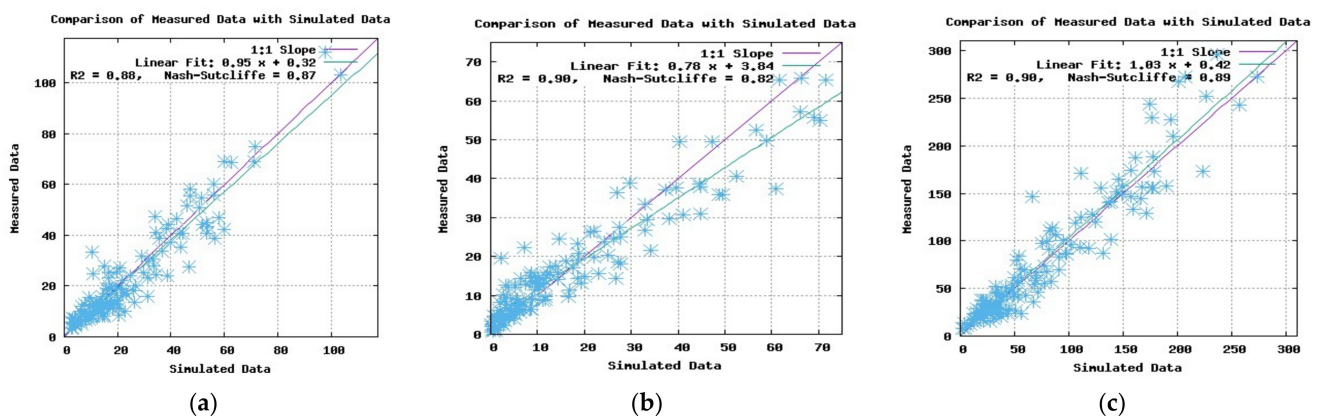


**Figure 2.** Scatter plot and objective functions for calibration period for (a) Choccolocco Creek at Jackson Shoal near Lincoln at USGS Gage 02404400, (b) Little Tallapoosa River near Newell near Newell at USGS Gage 24133000, and (c) Cahaba River near Marion Junction at USGS Gage 02425000.

While the model efficiency was good, SWAT produces poor simulation performance in dry seasons and for low flow situations. The research analyzed the lowest 10 percentile of flow for all three of the USGS gages used for the calibration (Figure 4). The scatter plots and objective functions showed that the model under-predicted streamflow discharge during

drought conditions or low flow situations. Low streamflow modeling and calibrations are better assessed specific models [62], over long calibration periods, and with a targeted multi-objective functions approach [63]. The ARB is a large basin, which has limited data for low flows, considering monthly simulation over the calibration period. Moreover, the research focused more on general streamflow changes, and SWAT model performance efficiency from the objective functions and goodness of fits of the hydrographs were high enough and appropriate for the climate change studies.

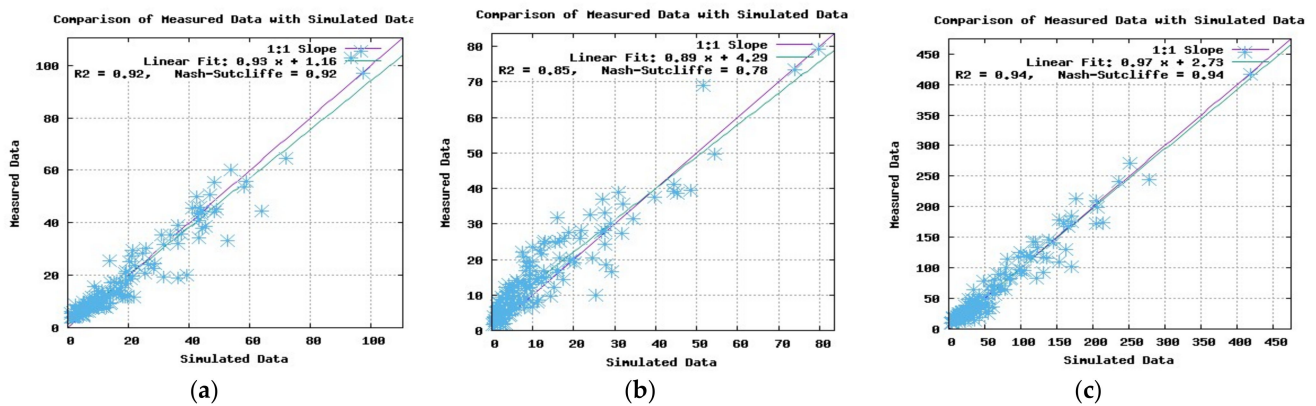


**Figure 3.** Scatter plot and objective functions for validation period for (a) Choccolocco Creek at Jackson Shoal near Lincoln at USGS Gage 02404400, (b) Little Tallapoosa River near Newell near Newell at USGS Gage 24133000, and (c) Cahaba River near Marion Junction at USGS Gage 02425000.

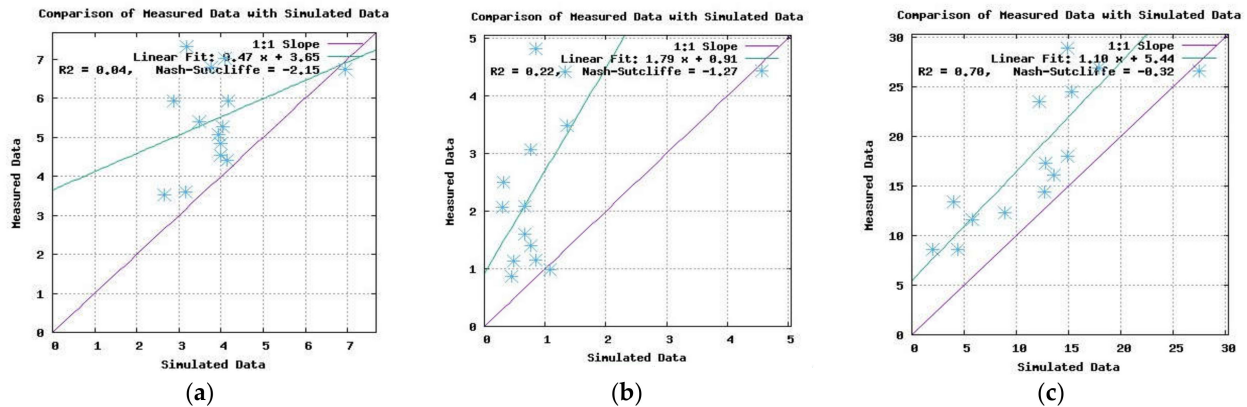


**Figure 4.** Scatter plot and objective functions for calibration of low flows (lower 10% percentile) for USGS gages (a) 02404400, (b) 24133000, and (c) 02425000.

The hydrographs (Figures 5–7) of the measured and simulated streamflow data for the calibration (1995–2005) and validation (1985–1995) periods show high goodness of fit and a reliable measure of the performance of the SWAT model.

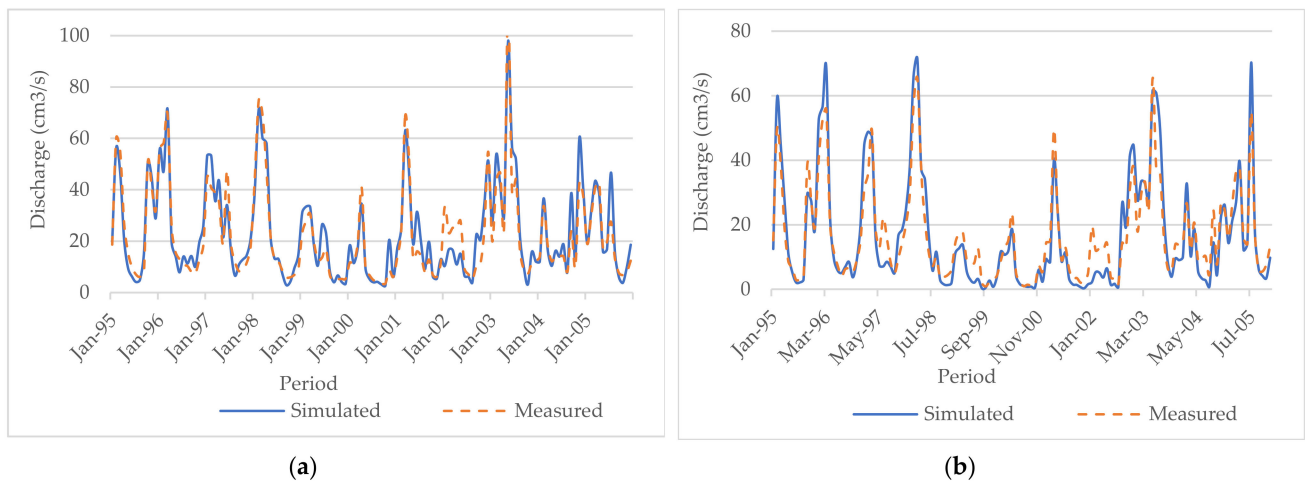


**Figure 5.** Monthly streamflow hydrographs for (a) calibration and (b) validation periods at USGS gage 02404400, on the Choccolocco Creek at Jackson Shoal near Lincoln.

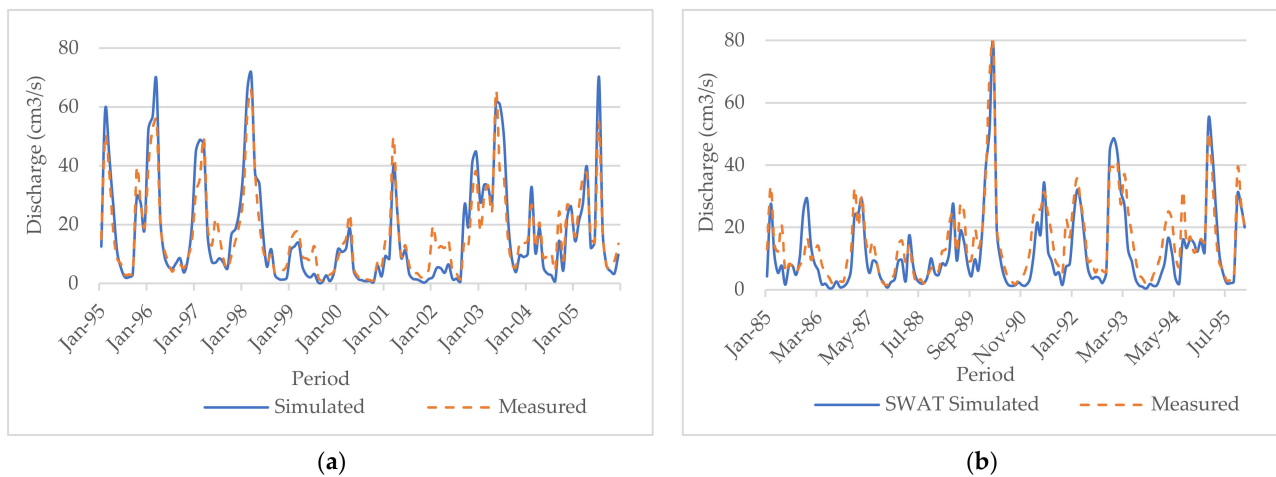


**Figure 6.** Monthly streamflow hydrographs for (a) calibration and (b) validation periods at USGS gage 02413300, on the Little Tallapoosa River near Newell.

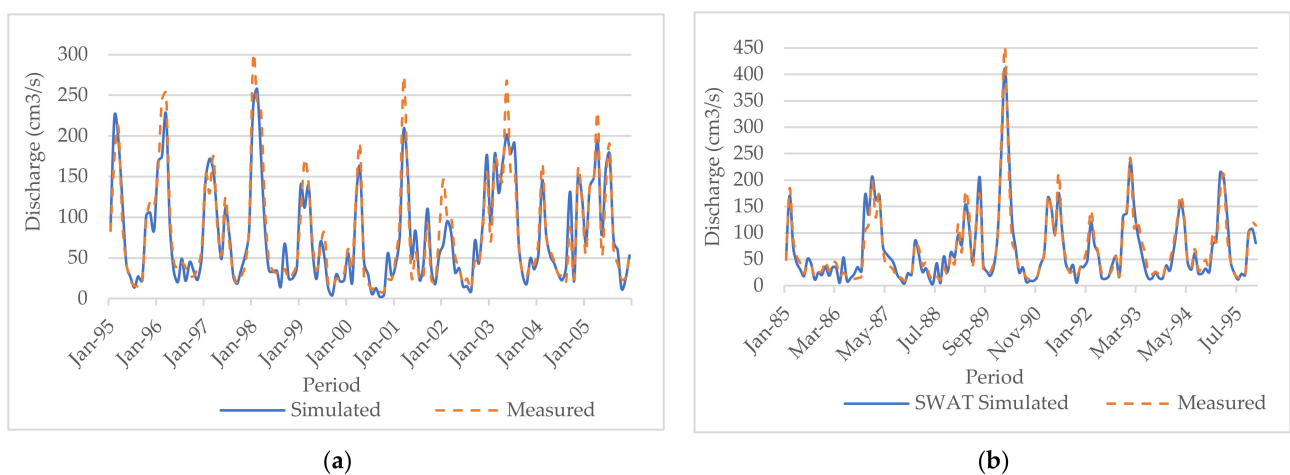


**Figure 7.** Monthly streamflow hydrographs for (a) calibration and (b) validation periods at USGS gage 02425000, on the Cahaba River near Marion Junction.

### 3.3. Analysis of Simulated Baseline against Future Streamflow

Figure 8a,b show the relative change in monthly streamflow discharge between 1980 baseline against 2045 and 2075 simulated streamflow discharge values, respectively. The majority of the relative changes ranged between  $-100\%$  and  $292\%$  for 2045 and 2075, with only HADGEM for June 2075 showing a higher change above  $421\%$ . There were decreased changes up to  $100\%$  in streamflow for winter months for almost all scenarios and years, and general increases for spring, summer, and fall seasons.

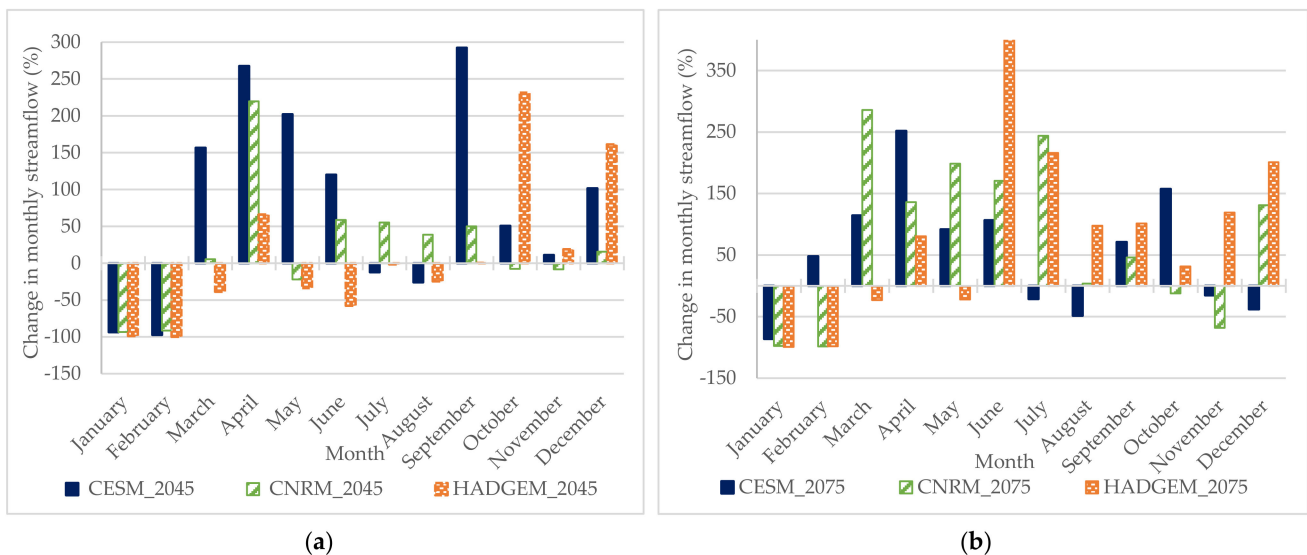


**Figure 8.** Percentage changes in monthly streamflow for 2045 (a) and 2075 (b) relative to 1980 baseline values.

Figures 9 and 10 show the simulated average monthly streamflow hydrographs and Tables 6 and 7 show the average monthly streamflow discharge for the years 2045 and 2075, for the three GCMs against that for 1980 (baseline). For the year 2045, average streamflow discharge based on CNRM-CM5 and HADGEM2-AO.1 GCMs showed decreased values compared to 1980 baseline values, while CESM1-BGC.1 simulated the highest increase in streamflow discharge. For the year 2075, streamflow simulations based on all three GCMs had higher/increased average annual streamflow discharge compared to 1980 baseline value. However, the different GCMs streamflow hydrographs for both 2045 and 2075 had higher monthly variabilities and peak flows compared to 1980 baseline values, especially in winter, spring, and fall months (Figures 9 and 10).

Seasonally, monthly streamflow increases between 50 and 250% were simulated for spring and autumn months with decreases in summer months for 2045. Spring and summer months for 2075 resulted in increased monthly streamflow between 50 and 300%, while autumn and spring months had decreased streamflow. The year 2075 is expected to have higher increased streamflow discharges with higher frequencies of variable peak flows. This result is unique to the research area and southern USA region, yet similar to other research findings that predicted future increases in temperature and moderate increases in precipitation will result in increases in future streamflow discharge and variability in average daily and monthly streamflow discharge [32]. While the results are prone to inherent uncertainties associated with the downscaling of the GCMs used, the hydrographs indicate that the ARB is likely to experience generally slight increase in streamflow discharge for 2045 and a relatively higher increase in 2075, especially during the winter and spring months, with higher frequencies in monthly peak flows.

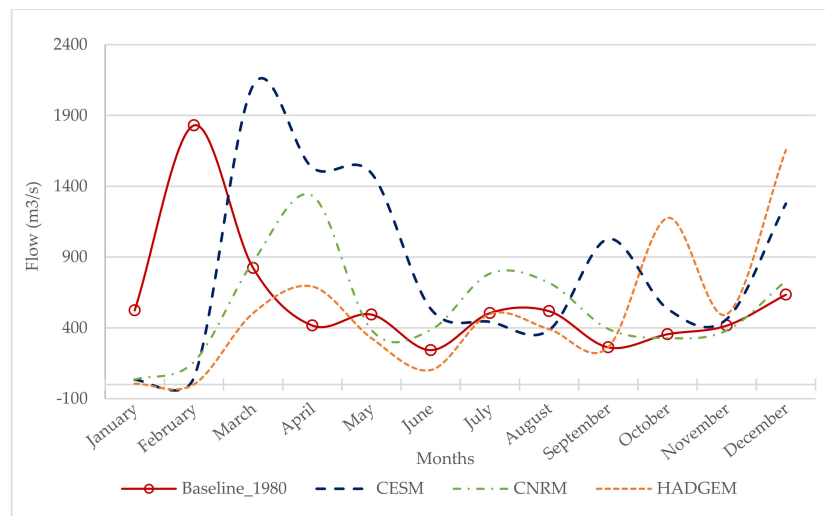


Figure 9. Simulated streamflow for1980 baseline and 2045 climate conditions.

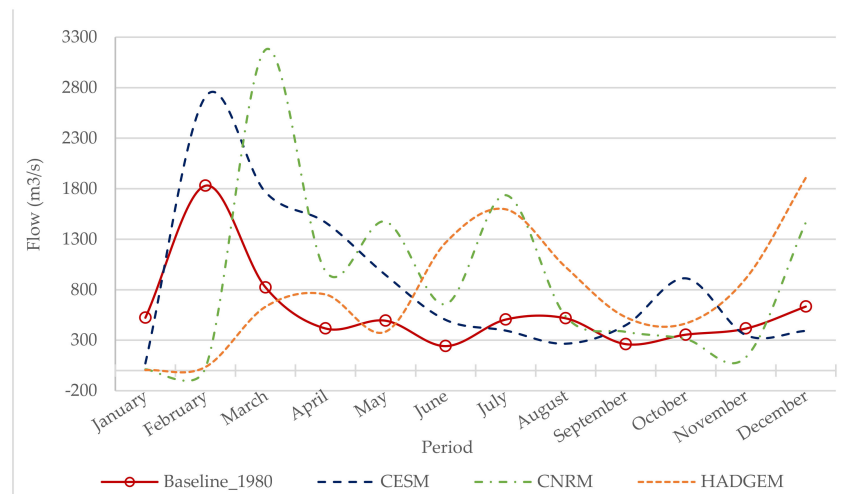


Figure 10. Simulated streamflow for1980 baseline and 2075 climate conditions.

Table 6. Comparison of simulated 1980 baseline monthly streamflow ( $m^3/s$ ) to 2045 streamflow from the different General Circulation Models (GCMs).

Months	Baseline	CESM ( $m^3/s$ )	CNRM ( $m^3/s$ )	HADGEM ( $m^3/s$ )
January	523.58	33.61	35.15	6.19
February	1829.83	48.65	160.30	1.39
March	823.17	2112.00	867.90	504.60
April	416.82	1532.00	1333.00	692.00
May	493.85	1491.00	385.10	327.20
June	242.73	534.40	385.40	102.40
July	504.61	443.00	783.30	497.20
August	517.92	384.50	717.70	390.80
September	261.99	1028.00	392.90	262.90
October	354.82	534.90	328.10	1176.00
November	415.98	461.90	381.40	495.20
December	634.01	1277.00	731.80	1656.00
Average	584.94	823.41	541.84	509.32
Percentage change to 1980 baseline		40.77	-7.37	-12.93
Correlation between baseline and GCMs		-0.18	-0.20	-0.22

**Table 7.** Comparison of simulated 1980 baseline monthly streamflow ( $\text{m}^3/\text{s}$ ) to 2075 streamflow from the different GCMs.

Months	1980 Baseline	CESM ( $\text{m}^3/\text{s}$ )	CNRM ( $\text{m}^3/\text{s}$ )	HADGEM ( $\text{m}^3/\text{s}$ )
January	523.58	71.79	11.42	4.73
February	1829.83	2710.00	25.84	35.61
March	823.17	1765.00	3176.00	632.00
April	416.82	1466.00	983.60	753.20
May	493.85	946.00	1474.00	384.80
June	242.73	501.70	657.00	1266.00
July	504.61	396.40	1736.00	1596.00
August	517.92	266.40	536.40	1024.00
September	261.99	448.30	382.80	528.40
October	354.81	913.10	311.50	466.80
November	415.98	351.40	132.10	911.20
December	634.01	392.50	1466.00	1908.00
Average	584.94	852.38	907.72	792.56
Percentage change to 1980 Baseline		45.72	55.18	35.49
Correlation between baseline and GCMs		0.79	−0.01	−0.35

#### 4. Conclusions

The goal of the study was to use an integrated modeling approach that assimilated downscaled climate data into the SWAT model to estimate hydrologic responses to future climatic variability and change within the ARB. The approach utilized data from three CMIP5 GCMs under the IPCC medium emission scenario (RCP 4.5). After calibration and validation, the SWAT model performed well in simulating historical streamflow within the ARB, although the model under-predicted streamflow during dry season and low flow conditions.

The projected climate conditions based on downscaled GCMs were compared to 1980 baseline conditions at a USGS gage within the watershed. This comparison indicated that HADGEM and CESM projected increases in average minimum and maximum temperature for the future climate conditions. Conversely, the CNRM model indicated that the climatic variables would exhibit lower values, specifically temperature and precipitation when compared to variables for the baseline year. In general, the research results indicate situations of likely periods of increase and decrease in streamflow and water availability during the periods from mid to end of the 21st century. It was projected that changes in future climate conditions within the ARB could result in positive and negative changes in monthly streamflow compared to the baseline years. It is expected that there would be a slight increase in annual streamflow in 2045 and a considerable increase in 2075, under medium emission scenario. The results indicate situations of likely increase and decrease in mean monthly streamflow discharge and increase in the frequency and variability in peak flows during the periods from mid to end of the 21st century. Seasonally, monthly streamflow increases between 50 and 250% were simulated for spring and autumn months with decreases in summer months for 2045. Spring and summer months for 2075 resulted in increased monthly streamflow between 50 and 300%, while autumn and spring months had decreased streamflow. As discussed earlier, the result is prone to inherent uncertainties associated with the downscaling techniques used to convert GCM model outputs to scales that are useful for hydrological modeling applications. Moreover, since SWAT underestimates low flows, this could have some level of uncertainty in the predicted changes in future streamflow variabilities.

Nevertheless, the findings indicate potential periods of both increased and decreased streamflow and resulting water availability impacts for the future mid and end of the century. Changing water budgets and availability including droughts and flooding situations could have adverse impacts on many sectors including agriculture, forestry, industries, and hydroelectric power systems. These potential impacts raise questions about the need for climate change adaptation to ensure efficient and sustainable management of water and

water-related disasters within the research watershed, Alabama, and the U.S. in general. The ARB is typical of many watersheds in the region; therefore, this study and results provide information on how similar watersheds might respond to future climate changes. Moreover, the study helps fill some of the research gaps and need for more information on how projected climate changes could impact water quantity in southeastern USA watersheds, specifically Alabama, which currently lacks studies related to climate changes.

**Author Contributions:** Conceptualization, J.E.Q., A.B.N., and S.F.; methodology, J.E.Q., S.F., and A.B.N.; software, A.B.N.; validation, J.E.Q. and A.B.N.; formal analysis, A.B.N., J.E.Q., and S.F.; investigation, J.E.Q. and A.B.N.; resources, A.B.N.; data curation, A.B.N.; writing—original draft preparation, A.B.N.; writing—review and editing, J.E.Q., A.B.N., S.F., R.A., and G.E.A.; visualization, J.E.Q. and S.F.; supervision, J.E.Q.; project administration, J.E.Q.; funding acquisition, J.E.Q. All authors have read and agreed to the published version of the manuscript.

**Funding:** This research supported by USDA–NIFA, grant number 1001194.

**Data Availability Statement:** Data can be found in the references cited in the manuscript.

**Acknowledgments:** We wish to thank Elizabeth Quansah for her review and contribution to improving the paper.

**Conflicts of Interest:** The authors declare no conflict of interest.

## References

1. UN General Assembly. United Nations Framework Convention on Climate Change (UNFCCC) (1992): Resolution Adopted by the General Assembly, 20 January 1994, A/RES/48/189. Available online: <https://www.refworld.org/docid/3b00f2770.html> (accessed on 12 June 2018).
2. IPCC. *Climate Change 2001: Synthesis Report. A Contribution of Working Groups I, II, and III to the Third Assessment Report of the Intergovernmental Panel on Climate Change*; Watson, R.T., the Core Writing Team, Eds.; Cambridge University Press: Cambridge, UK; New York, NY, USA, 2001; p. 398.
3. IPCC. *IPCC Special Report on Climate Change, Desertification, Land Degradation, Sustainable Land Management, Food Security, and Greenhouse Gas Fluxes in Terrestrial Ecosystems: Summary for Policymakers*. 2019. Available online: [https://www.ipcc.ch/site/assets/uploads/2019/08/4-SPM\\_Approved\\_Microsite\\_FINAL.pdf](https://www.ipcc.ch/site/assets/uploads/2019/08/4-SPM_Approved_Microsite_FINAL.pdf) (accessed on 5 April 2019).
4. NASA. Scientific Consensus: Earth’s Climate is Warming. Available online: <https://climate.nasa.gov/scientific-consensus/> (accessed on 19 November 2020).
5. NASA Goddard Institute for Space Studies (GISS): Facts. 2020. Available online: <https://climate.nasa.gov/vital-signs/global-temperature/> (accessed on 1 November 2020).
6. Allen, M.R.; Dube, O.P.; Solecki, W.; Aragón-Durand, F.; Cramer, W.; Humphreys, S.; Kainuma, M.; Kala, J.; Mahowald, N.; Muloggetta, Y.; et al. *Framing and Context*. In *Global Warming of 1.5 °C. An IPCC Special Report on the Impacts of Global Warming of 1.5 °C above Pre-Industrial Levels and Related Greenhouse Gas Emission pathways, in the Context of Strengthening the Global Response to the Threat of Climate Change, Sustainable Development, and Efforts to Eradicate Poverty*; Masson-Delmotte, V., Zhai, P., Pörtner, H.-O., Roberts, D., Skea, J., Shukla, P.R., Pirani, A., Moufouma-Okia, W., Péan, C., Pidcock, R., et al., Eds.; The Intergovernmental Panel on Climate Change: Geneva, Switzerland, 2018.
7. Seneviratne, S.I.; Nicholls, N.; Easterling, D.; Goodess, C.M.; Kanae, S.; Kossin, J.; Luo, Y.; Marengo, J.; McInnes, K.; Rahimi, M.; et al. Changes in climate extremes and their impacts on the natural physical environment. In *Managing the Risks of Extreme Events and Disasters to Advance Climate Change Adaptation*; Field, C.B.V., Barros, T.F., Stocker, D., Qin, D.J., Dokken, K.L., Ebi, M.D., Mastrandrea, K.J., Mach, G.-K., Plattner, S.K., Allen, M., Eds.; A Special Report of Working Groups I and II of the Intergovernmental Panel on Climate Change (IPCC); Cambridge University Press: Cambridge, UK; New York, NY, USA, 2012; pp. 109–230.
8. IPCC. *Climate Change Synthesis Report Summary Chapter for Policymakers*; IPCC: Geneva, Switzerland, 2014.
9. UNESCO. *The impact of global change on water resources: The Response of UNESCO’s International Hydrologic Programme*; Division of Water Sciences: Paris, France, 2011. Available online: <https://unesdoc.unesco.org/ark:/48223/pf0000192216> (accessed on 5 December 2020).
10. Bates, B.C.; Kundzewicz, Z.W.; Wu, S.; Palutikof, J.P. (Eds.) *Climate Change and Water. Technical Paper of the Intergovernmental Panel on Climate Change*; IPCC Secretariat: Geneva, Switzerland, 2008.
11. Gleick, P.H. Water- The potential consequences of climate variability and change for the water resources of the United States. In *The Report of the Water Sector Assessment Team of the National Assessment of the Potential Consequences of Climate Variability and Change for the U.S. Global Change Research Program*; Peter, H.G., Ed.; Pacific Institute for Studies in Development, Environment, and Security: Oakland, CA, USA, 2000; pp. 126–151. ISBN 1-893790-04-5.

12. U.S. Environmental Protection Agency (EPA). *Climate Change Indicators in the United States*, 4th ed.; EPA 430-R-16-004; 2016. Available online: [www.epa.gov/climate-indicators](http://www.epa.gov/climate-indicators) (accessed on 20 May 2020).
13. Weiskopf, S.R.; Rubenstein, M.A.; Crozier, L.G.; Gaichas, S.; Griffis, R.; Halofsky, J.E.; Hyde, K.J.W.; Morelli, T.L.; Morissette, J.T.; Muñoz, R.C.; et al. Climate change effects on biodiversity, ecosystems, ecosystem services, and natural resource management in the United States. *Sci. Total Environ.* **2000**, *733*. [[CrossRef](#)] [[PubMed](#)]
14. Pitz, C.F. Predicted Impacts of Climate Change on Groundwater Resources of Washington State. Department of Ecology, The State of Washington. Report No. 16-03-006; 2016. Available online: <https://fortress.wa.gov/ecy/publications/documents/1603006.pdf> (accessed on 7 April 2019).
15. Vincent, W.F. *Effects of Climate Change on Lakes*; Elsevier Inc.: Quebec City, QC, Canada, 2009; pp. 55–60.
16. Lins, H.F. *USGS Hydro-Climatic Data Network 2009 (HCDN-2009)*; U.S. Geological Survey Fact Sheet 2012-3047; U.S. Geological Survey: Reston, VA, USA, 2009. Available online: <https://pubs.usgs.gov/fs/2012/3047/pdf/fs2012-3047.pdf> (accessed on 8 June 2020).
17. U.S. Geological Survey (USGS). *Analysis of Data from the National Water Information System*; U.S. Geological Survey (USGS): Reston, VA, USA, 2006.
18. Hoegh-Guldberg, O.; Jacob, D.; Taylor, M.M.; Bindi, M.; Brown, S.; Camilloni, I.; Diedhiou, A.; Djalante, R.; Ebi, K.L.; Engelbrecht, F.; et al. Impacts of 1.5 °C global warming on natural and human systems. In *Global Warming of 1.5 °C. An IPCC Special Report on the Impacts of Global Warming of 1.5 °C above Pre-Industrial Levels and Related Global Greenhouse Gas Emission Pathways, in the Context of Strengthening the Global Response to the Threat of Climate Change, Sustainable Development, and Efforts to Eradicate Poverty*; Masson-Delmotte, V., Zhai, P., Pörtner, H.-O., Roberts, D., Skea, J., Shukla, P.R., Pirani, A., Moufouma-Okia, W., Péan, C., Pidcock, R., et al., Eds.; 2018; In Press.
19. Ali, R.; Kuriqi, A.; Abubaker, S.; Kisi, O. Long-Term Trends and Seasonality Detection of the Observed Flow in Yangtze River Using Mann-Kendall and Sen's Innovative Trend Method. *Water* **2019**, *11*, 1855. [[CrossRef](#)]
20. Kuriqi, A.; Ali, R.; Pham, Q.B.; Gambini, J.M.; Gupta, V.; Malik, A.; Linh, N.T.T.; Joshi, Y.; Anh, D.T.; Dong, X.; et al. Seasonality shift and streamflow flow variability trends in central India. *Acta Geophys.* **2020**, *68*, 1461–1475. [[CrossRef](#)]
21. Pathak, T.; Maskey, M.; Dahlberg, J.; Kearns, F.; Bali, K.; Zaccaria, D. Climate change trends and impacts on California agriculture: A detailed review. *Agronomy* **2018**, *8*, 25. [[CrossRef](#)]
22. Mirzabaev, A.; Wu, J.; Evans, J.; García-Oliva, F.; Hussein, I.A.G.; Iqbal, M.H.; Kimutai, J.; Knowles, T.; Meza, F.; Nedjraoui, D.; et al. Desertification. In *Climate Change and Land: An IPCC Special Report on Climate Change, Desertification, Land Degradation, Sustainable Land Management, Food Security, and Greenhouse Gas Fluxes in Terrestrial Ecosystems*; Shukla, P.R., Skea, J., Calvo Buendia, E., Masson-Delmotte, V., Pörtner, H.-O., Roberts, D.C., Zhai, P., Slade, R., Connors, S., van Diemen, R., et al., Eds.; IPCC: Geneva, Switzerland, 2019.
23. IPCC. *Climate Change 2014: Synthesis Report Summary for Policymakers*. Contribution of Working Groups I, II and III to the Fifth Assessment Report of the Intergovernmental Panel on Climate Change. Available online: [https://www.ipcc.ch/site/assets/uploads/2018/02/AR5\\_SYR\\_FINAL\\_SPM.pdf](https://www.ipcc.ch/site/assets/uploads/2018/02/AR5_SYR_FINAL_SPM.pdf) (accessed on 12 August 2020).
24. Randall, D.A.; Wood, R.A.; Bony, S.; Colman, R.; Fichefet, T.; Fyfe, J.; Kattsov, V.; Pitman, A.; Shukla, J.; Srinivasan, J.; et al. *Climate Models and Their Evaluation*; Cambridge University Press: Cambridge, UK, 2007.
25. Alexander, L.V.; Arblaster, J.M. Historical and projected trends in temperature and precipitation extremes in Australia in observations and CMIP5. *Weather Clim. Extremes* **2017**, *34–56*. [[CrossRef](#)]
26. Li, Z.; Jin, J. Evaluating climate change impacts on streamflow variability based on a multisite multivariate GCM downscaling method. *Hydrol. Earth Syst. Sci. Discuss.* **2017**, *1–22*. [[CrossRef](#)]
27. Miao, C.; Duan, Q.; Sun, Q.; Huang, Y.; Kong, D.; Yang, T.; Gong, W. Assessment of CMIP5 climate models and projected temperature changes over Northern Eurasia. *Environ. Res. Lett.* **2004**, *9*. [[CrossRef](#)]
28. Koch, J.; Cornelissen, T.; Fang, Z.; Bogen, H.; Diekkrüger, B.; Kollet, S.; Stisen, S. Inter-comparison of three distributed hydrological models with respect to seasonal variability of soil moisture patterns at a small forested catchment. *J. Hydrol.* **2016**, *533*, 234–249. [[CrossRef](#)]
29. Leta, O.T.; El-Kadi, A.I.; Dulai, H.; Ghazal, K.A. Assessment of climate change impacts on water balance components of Heeia watershed in Hawaii. *J. Hydrol. Reg. Stud.* **2016**, *8*, 182–197. [[CrossRef](#)]
30. Mohammed, I.N.; Bombles, A.; Wemple, B.C. The use of CMIP5 data to simulate climate change impacts on flow regime within the Lake Champlain Basin. *J. Hydrol. Reg. Stud.* **2016**, *3*, 160–186. [[CrossRef](#)]
31. Sunde, M.G.; He, H.S.; Hubbart, J.A.; Urban, M.A. Integrating downscaled CMIP5 data with a physically based hydrologic model to estimate potential climate change impacts on streamflow processes in a mixed-use watershed. *Hydrol. Proc.* **2017**, *31*, 1790–1803. [[CrossRef](#)]
32. Su, B.; Huang, J.; Zeng, X.; Gao, C.; Jiang, T. Impacts of climate change on streamflow in the upper Yangtze River basin. *Clim. Change* **2017**, *141*, 533–546. [[CrossRef](#)]
33. Kleinschmidt, E. Alabama River Basin Management Plan. 2005. Available online: <http://www.adem.state.al.us/programs/water/nps/files/AlabamaBMP.pdf> (accessed on 4 July 2020).
34. Murgulet, D.G.; Tick, G. The extent of saltwater intrusion in southern Baldwin County, Alabama. *Environ. Geol.* **2008**, *55*, 1235–1245. [[CrossRef](#)]

35. Sinclair, W.C. Sinkhole development resulting from ground water withdrawal in the Tampa Area, Florida. In *USGS Water-Resources Investigations Report 81-50*; 1982. Available online: <https://pubs.usgs.gov/wri/1981/0050/report.pdf> (accessed on 14 June 2020).
36. Runkle, J.; Kunkel, K.; Stevens, L.; Frankson, R. Alabama State climate summary. In *NOAA Technical Report NESDIS 149-AL*; March 2019 Revision; Auburn University: Auburn, AL, USA, 2017; 4 pp.
37. Karl, T.R.; Melillo, J.M.; Peterson, T.C. Global Climate Change Impacts in the United States. 2009; Volume 54. Available online: [www.globalchange.gov/usimpacts](http://www.globalchange.gov/usimpacts) (accessed on 12 August 2018).
38. IPCC. *Summary for Policymakers: Managing the Risks of Extreme Events and Disasters to Advance Climate Change Adaptation*; Field, C.B.V., Barros, T.F., Stocker, D., Qin, D.J., Dokken, K.L., Ebi, M.D., Mastrandrea, K.J., Mach, G.-K., Plattner, S.K., Allen, M., Eds.; A Special Report of Working Groups I and II of the Intergovernmental Panel on Climate Change; Cambridge University Press: Cambridge, UK; New York, NY, USA, 2012; pp. 14–15.
39. U.S. Army Corps of Engineers (USACE). *Environmental Data Inventory, State of Alabama: Mobile, Alabama*; USACE: Washington, DC, USA, 1998.
40. Gangrade, S.; Kao, S.-C.; McManamay, R.A. Multi-model Hydroclimate Projections for the Alabama-Coosa-Tallapoosa River Basin in the Southeastern United States. *Nat. Res. Sci. Rep.* **2020**, *10*. [[CrossRef](#)] [[PubMed](#)]
41. Arnold, J.G.; Srinivasan, R.; Muttiah, R.S.; Williams, J.R. Large area hydrologic modeling and assessment part I: Model development. *J. Am. Water Resour. Assoc.* **1998**, *34*, 73–89. [[CrossRef](#)]
42. Krysanova, V.; White, M. Advances in water resources assessment with SWAT—An overview. *Hydrol. Sci. J.* **2015**, *60*, 771–783. [[CrossRef](#)]
43. Neitsch, S.L.; Arnold, J.G.; Kiniry, J.R.; Srinivasan, R.; Williams, J.R. *Soil and Water Assessment Tool, User Manual, Version 2000*; Grassland, Soil and Water Research Laboratory-Agricultural Research Service: Temple, TX, USA. Available online: <https://swat.tamu.edu/media/1294/swatuserman.pdf> (accessed on 8 January 2019).
44. Bennett, J.C.; Grose, M.R.; Corney, S.P.; White, C.J.; Holz, G.K.; Katzfey, J.J.; Post, D.A.; Bindoff, N.L. Performance of an empirical bias-correction of a high-resolution climate dataset. *Int. J. Climatol.* **2014**, *34*, 2189–2204. [[CrossRef](#)]
45. Aryal, Y.; Zhu, J. Multimodel ensemble projection of meteorological drought scenarios and connection with climate based on spectral analysis. *Int. J. Climatol.* **2020**, *40*, 3360–3379. [[CrossRef](#)]
46. Zhao, T.; Dai, A. The magnitude and causes of global drought changes in the twenty-first century under a low–moderate emissions scenario. *J. Clim.* **2015**, *28*, 4490–4512. [[CrossRef](#)]
47. Rupp, D.E. An evaluation of 20th century climate for the Southeastern United States as simulated by Coupled Model Intercomparison Project Phase 5 (CMIP5) global climate models. U.S. Geological Survey Open-File Report; U.S. Geological Survey: Reston, VA, USA, 2016; 32 p. [[CrossRef](#)]
48. Voldoire, A.; Sanchez-Gomez, E.; Salas, D.; Méliá, Y.; Decharme, B.; Cassou, C.; Sénési, S.; Valcke, S.; Beau, I.; Alias, A.; et al. The CNRM-CM5.1 global climate model: Description and basic evaluation. *Clim. Dyn.* **2011**, *40*, 2091–2121. [[CrossRef](#)]
49. Long, M.C.; Lindsay, K.S.; Peacock, S.; Moore, J.K.; Doney, S.C. Twentieth-Century Oceanic Carbon Uptake and Storage in CESM1(BGC). *J. Clim.* **2013**, *26*, 6775–6800. [[CrossRef](#)]
50. Bellouin, N.; Collins, W.J.; Culverwell, I.D.; Halloran, P.R.; Hardiman, S.C.; Hinton, T.J.; Jones, C.D.; McDonald, R.E.; McLaren, A.J.; O'Connor, F.M.; et al. The HadGEM2 family of Met Office Unified Model climate configurations. *Geosci. Model Devel.* **2011**, *4*, 723–757.
51. Thomson, A.M.; Calvin, K.V.; Smith, S.J.; Kyle, G.P.; Volke, A.; Patel, P.; Delgado-Arias, S.; Bond-Lamberty, B.; Wise, M.A.; Clarke, L.E.; et al. RCP4.5: A pathway for stabilization of radiative forcing by 2100. *Clim. Chang.* **2011**, *109*, 77. [[CrossRef](#)]
52. Maurer, E.P. Uncertainty in hydrologic impacts of climate change in the Sierra Nevada, California under two emissions scenarios. *Clim. Chang.* **2007**, *82*, 309–325. [[CrossRef](#)]
53. Quansah, J.E.; Engel, B.A.; Chaubey, I. Tillage Practices Usage in Early Warning Prediction of Atrazine Pollution. *Transac. ASABE* **2008**, *51*, 1311–1321. [[CrossRef](#)]
54. Arnold, J.G.; Moriasi, D.N.; Gassman, P.W.; Abbaspour, K.C.; White, M.J.; Srinivasan, R.; Santhi, C.; Harmel, R.D.; van Griensven, A.; Van Liew, N.W.; et al. SWAT: Model use, calibration, and validation. *Trans. ASABE* **2012**, *55*, 1491–1508. [[CrossRef](#)]
55. Nash, J.E.; Sutcliffe, J.V. River flow forecasting through conceptual models: Part 1. A discussion of principles. *J. Hydrol.* **1970**, *10*, 282–290. [[CrossRef](#)]
56. Moriasi, D.N.; Arnold, J.G.; Van Liew, M.W.; Bingner, R.L.; Harmel, R.D.; Veith, T.L. Model evaluation guidelines for systematic quantification of accuracy in watershed simulations. *Trans. ASABE* **2007**, *50*, 885–900. [[CrossRef](#)]
57. Krause, P.; Boyle, D.P.; Base, F. Comparison of different efficiency criteria for hydrological model assessment. *Adv. Geosci.* **2005**, *5*, 89–97. [[CrossRef](#)]
58. McCuen, R.H. Assessment of Hydrological and statistical significance. *J. Hydrol. Eng. ASCE* **2016**, *21*. [[CrossRef](#)]
59. Mann, H.B. Nonparametric tests against trend. *Econometrica* **1945**, *13*, 245–259. [[CrossRef](#)]
60. Sen, P. Estimated of the regression coefficient based on Kendall's Tau. *J. Am. Stat. Assoc.* **1968**, *39*, 1379–1389. [[CrossRef](#)]
61. Theil, H. A rank-invariant method of linear and polynomial regression analysis, I, II, III. In *Henri Theil's Contributions to Economics and Econometrics*; Volume 23, Springer: Dordrecht, The Netherlands, 1992. [[CrossRef](#)]

- 
62. Parra, V.; Arumí, J.L.; Muñoz, E. Identifying a Suitable Model for Low-Flow Simulation in Watersheds of South-Central Chile: A Study Based on a Sensitivity Analysis. *Water* **2019**, *11*, 1506. [[CrossRef](#)]
  63. Garcia, F.; Folton, N.; Oudin, L. Which objective function to calibrate rainfall–runoff models for low-flow index simulations? *Hydrol. Sci. J.* **2017**. [[CrossRef](#)]